Intrinsic Catalytic Cracking Activity of Hexane over H−ZSM-5, H−β and H−Y Zeolites

S. Kotrel, M. P. Rosynek, and J. H. Lunsford*

Department of Chemistry, Texas A&M University, College Station, Texas 77843

Received: June 8, 1998; In Final Form: November 16, 1998

Mono- and bimolecular intrinsic rate constants for the conversion of *n*-hexane over H−Y, H−ZSM-5, and H−β zeolites were measured at 623 K by combining conventional catalytic techniques with gravimetric adsorption measurements. Since H-zeolites are catalytically active, their adsorption properties under reaction conditions could not be directly obtained. Rather, adsorption experiments were carried out on the H-zeolites at temperatures below the onset of catalytic activity (450−530 K). Thermodynamic adsorption constants for the H forms at 623 K were then obtained by extrapolation. In addition, the catalytically inactive Na forms were chosen to characterize the overall temperature dependence of *n*-hexane adsorption on ZSM-5, Y, and β zeolites in the range 450−623 K. For the cracking experiments, monomolecular conditions were ensured by choosing a low hexane pressure (<0.57 kPa) and short contact times. The intrinsic activity for mono- and bimolecular *n*-hexane cracking over the zeolites, after taking into account the amounts of adsorbed hydrocarbon, was in the order H−ZSM-5 > H−β > dealuminated H−Y ≫ H−Y.

Introduction

Acidic zeolites are widely used as catalysts for such commercial processes as the cracking of petroleum. Although it is generally agreed that Brönsted acid centers are involved in these reactions, attempts to relate the number of protons and their acid strength to a particular catalytic reaction have often led to inconsistent results. This is particularly the case when one compares the catalytic properties of different types of zeolites. As noted by Haag,[1] the difficulty in making comparisons may result from the fact that the concentration effect is not adequately treated. That is, zeolites have different adsorption characteristics that will influence the local concentration of hydrocarbons within the cavities or channels. This enhancement in reactant concentration, relative to the gas phase, may be viewed as an enrichment factor.

Haag[1] further recognized the importance of the adsorption enthalpy when considering the apparent activation energies for the cracking of a series of linear alkanes over an H−ZSM-5 zeolite. By applying the relationship

$$E_{app} = E_0 + \Delta H_{ads} \quad (1)$$

where E_{app} is the observed activation energy, E_0 is the intrinsic activation energy, and ΔH_{ads} is the enthalpy of adsorption, he was able to show that the value of E_0 was nearly constant, even though E_{app} varied by more than a factor of 2 in going from butane to decane. Similar results were obtained by Lercher and co-workers[2] for the cracking of propane through hexane. It should be noted that eq 1 applies only at low coverages and with first-order kinetics.

If one wishes to compare substantially different acid catalysts (e.g., different types of zeolites) based on their cracking activities, one has to keep in mind that the apparent activity is not a sufficient probe for the intrinsic acidity of these materials.[1] The cracking activity for a particular hydrocarbon over an acid catalyst is a function of the amount of the hydrocarbon adsorbed in the material, as well as the number and strength of the acid sites.[3,4]

In the present study, kinetic and adsorption data for the zeolites Y, ZSM-5, and beta (β),which are three important structures, were obtained in order to determine the intrinsic catalytic behavior of these materials for *n*-hexane cracking. The catalytic results were measured at temperatures near 623 K, which was sufficiently low for obtaining reliable adsorption data. To overcome the problem of reaction during adsorption measurements, two different approaches were used. First, *n*-hexane adsorption was measured on the inactive sodium form of the zeolites at temperatures up to 623 K, and second, the hydrogen form of the zeolites was used at sufficiently low temperature so that cracking did not occur. The results of adsorption on the hydrogen forms were then extrapolated to the reaction temperature using heats of adsorption.

The catalytic activities were measured under both unimolecular and bimolecular conditions. In the former case, direct protonation of the paraffin is believed to result in the cracking reaction, whereas in the latter case, secondary reactions between *n*-hexane and surface carbenium ions become significant. The two regimes were achieved by operating at very different hydrocarbon pressures, with lower pressures favoring the unimolecular reaction.

Experimental Section

Materials and Catalyst Preparation. H−β (PQ Corp.,-VALFOR CP-811Al-25), H−ZSM-5 (PQ Corp., CBV 5020 E), dealuminated H−Y (Linde, Y-84 C 1523732), and H−Y (Linde, LZ-Y52) zeolites were transformed into their ammonium forms by ion exchange. Approximately 20 g of the zeolite were exchanged in 500 mL of a 1 M NH_4NO_3 solution 6 times for 8 h at 358 K. The sodium forms were obtained by ion exchange of the materials with a 1 M NaCl solution 6 times for 8 h at 358 K. *n*-Hexane (99+%) was purchased from Janssen Chemica. The zeolites were pretreated by heating them in situ in flowing, dry N_2 at 373, 473, 573, and 673 K for 1 h at each step. Between steps the heating rate was 5 K min^{-1}.

Characterization. The catalysts were analyzed for Na and Al by first dissolving the zeolites in hydrofluoric acid. The

10.1021/jp982538l CCC: $18.00
Published on Web 01/15/1999

resulting solutions were analyzed by atomic absorption spectroscopy (AAS) using either the inductively coupled plasma (ICP) technique (Al^{3+}) or the flame technique (Na^{+}). Standard solutions were provided by Aldrich. The framework aluminum concentration was determined by ^{29}Si and ^{27}Al NMR and X-ray diffraction (XRD) for the Y-type zeolites. X-ray diffraction provided the unit cell parameters of the zeolites relative to Si, which was used as an internal standard. The number of framework aluminum atoms per unit cell, N_{Al}, was then calculated using the equation[5]

$$N_{Al} = 107.1(a_0 - 24.238) \quad (2)$$

where a_0 is the unit cell parameter. ^{29}Si and ^{27}Al NMR spectra were obtained with a Bruker MSL-300 spectrometer (7.05 T). To reduce the effects of quadrupolar interaction in ^{27}Al spectra, the samples were hydrated by storing them over a saturated NH_4NO_3 solution for 16 h. The presence of water in the zeolite results in a more symmetrical tetrahedral Al that is required for quantitative determination of framework aluminum. For the measurements, a zirconium rotor was filled with ca. 0.2 g of zeolite and the sample was spun (3.5 kHz) at the magic angle to remove line broadening caused by homonuclear and heteronuclear interactions. ^{29}Si and ^{27}Al spectra were obtained after 3000 or 1000 accumulations, respectively. From the ^{29}Si spectra the Si/Al ratio was calculated using the method of Lippmaa et al.[6] For β and ZSM-5 samples, the spectra were first deconvoluted following the peak assignments of Pariente et al.[7] and Axon et al.,[8] respectively. The intensity of the narrow line at 60 ppm in the ^{27}Al spectra was used to determine Al concentrations, from which Si/Al ratios were determined. A ZSM-5 sample, obtained from Mobil Oil Co., of a known Si/Al ratio and without extraframework Al, was used as an external standard.

Sorption Measurements. The sorption isotherms were determined gravimetrically using a Cahn RG vacuum microbalance system with the sample at temperatures in the range 433−523 K for H forms and 453−623 K for the Na forms of the zeolites, respectively. Prior to adsorption, the samples were outgassed by heating them in a dry N_2 stream stepwise to 373, 473, 573, and 673 K. The temperature was maintained for 1 h at each temperature and was increased at a rate of 5 K/min between temperatures. After evacuation of the N_2 and stabilization of the pressure at 10^{-3} Pa, the sample was allowed to cool to the temperature of the adsorption measurement. *n*-Hexane was then dosed into the system and allowed to equilibrate with the zeolite. The system was considered to be in equilibrium when the recorded pressure and sample weight remained stable for 20 min. To exclude any diffusion-related effects, in a separate experiment *n*-hexane was dosed at 423 K to each zeolite and the sample weight was recorded for 24 h. A long-term change in the sample weight was not observed.

The experimental isotherms were plotted as the uptake of the hydrocarbon, based on the weight of the dehydrated sample, versus the hexane pressure. The experimental data were then fit with a Langmuir model, using the method of least-squares errors. The accuracy of this fit was calculated by the average error (Δ), defined as

$$\Delta\,(\%) = \frac{100}{n_{exp}} \sum_{i=1}^{n_{exp}} \frac{(N_i^{exp} - N_i^{calc})}{N_i^{exp}} \quad (3)$$

where n_{exp} is the number of experiments, N_i^{exp} is the measured *n*-hexane uptake of the *i*th experiment, and N_i^{calc} is the calculated *n*-hexane uptake of the *i*th experiment.

TABLE 1: Na Content and Si/Al Ratios for H−ZSM-5, H−β, Dealuminated H−Y, and H−Y Zeolites

		Si/Al ratio			
catalyst	Na^+ (wt %)	^{29}Si NMR	^{27}Al NMR	XRD	Al_{tot}[a]
ZSM-5	0.08	42.1	35.0		25.9
β	0.05	18.7	16.6		12.8
deal. Y	0.03	4.9	8.8	4.3−4.7	3.4
Y	0.09	2.4		2.6−3.0	2.3

[a] Based on total aluminum analysis.

Catalytic Experiments. The cracking reactions were carried out in a conventional plug flow reactor consisting of a fused quartz tube with an internal diameter of 3, 4, or 6 mm (depending on the catalyst volume). A stream of N_2 (65 mL/min) was then passed through an *n*-hexane saturator at 273 K and, when necessary, was diluted with pure N_2 before it was allowed to enter the reactor.

The catalyst was pressed (100 MPa), sieved (20−40 mesh size), and then placed on top of a layer of fused quartz chips, which was held in place by a plug of quartz wool. Since the reactor was operating in an up-flow mode, the layer of quartz chips also functioned as a preheating zone for the feed gas. Prior to the experiment, the sample was pretreated as described for the sorption experiments. The reaction products were analyzed by GC (Hewlett-Packard model 5890 with an Al_2O_3/KCl-coated fused silica capillary column or a Varian GC model 3700 with a packed *n*-octane/Porasil column). The conversion was determined by comparing the *n*-hexane depletion during the cracking reaction with the *n*-hexane concentration with the reactor bypassed.

The rate constants were determined at *n*-hexane partial pressures of 5.3 kPa and <0.5 kPa. Since *n*-hexane cracking at 5.3 kPa led to a considerable deactivation of the samples due to coke formation, the exit gas stream was analyzed after 0.4 min time on stream and in 12 min intervals thereafter. Initial conversion and product selectivities were obtained by extrapolating the results to zero time on stream. When the *n*-hexane partial pressure was less than 0.5 kPa, the catalytic activity did not decrease with time on stream, provided that the contact time and thus the conversion were sufficiently low. An extrapolation was not necessary in this case. To obtain activation energies during monomolecular cracking, the reaction temperature was varied in the range 623−773 K, with an *n*-hexane pressure of 0.25 kPa.

Results and Discussion

Catalyst Characterization. The results for the Si/Al ratios of all zeolite samples are given in Table 1. The Si/Al ratios obtained by chemical analysis are based on the total aluminum content of the materials. The ratios calculated from XRD and ^{29}Si and ^{27}Al NMR reflect the framework aluminum concentration. As expected, similar Si/Al ratios from the total (AAS) and the framework aluminum (XRD,^{29}Si) content were determined for the H−Y zeolite. This confirms that only a small amount of extraframework aluminum was present. In the case of the dealuminated Y zeolite, ^{27}Al NMR underestimated the framework aluminum concentration because of the strong quadrupolar interaction caused by the highly distorted lattice of this material.[9] The Si/Al ratios calculated by XRD and ^{29}Si are significantly larger than the total Si/Al ratio due to the presence of a large amount of extraframework aluminum. The preferred values are those obtained by ^{29}Si NMR.

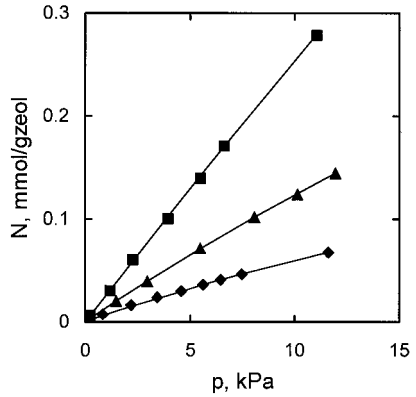

Figure 1. Adsorption isotherms for *n*-hexane on (■) Na−*β*, (▲) Na−Y, and (◆) Na−ZSM-5 zeolites at 623 K.

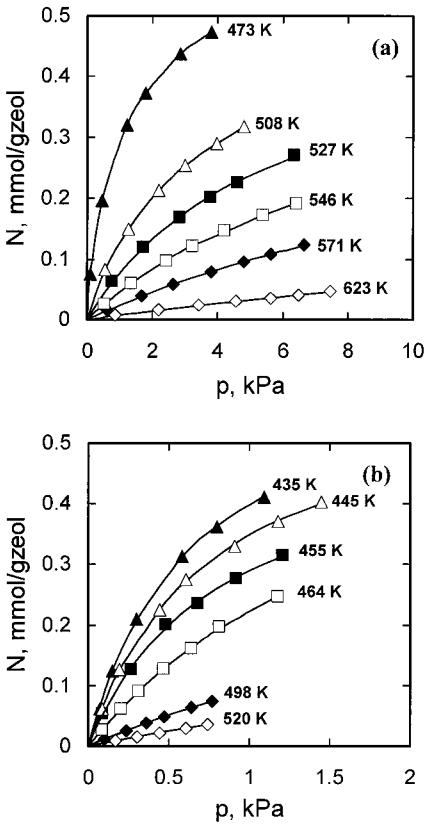

Figure 2. Adsorption isotherms for *n*-hexane on (a) Na−ZSM-5 in the range 473−623 K and (b) H−ZSM-5 in the range 435−520 K.

Since the Al concentration in the ZSM-5 and *β* samples is low and the ^{29}Si spectra are dominated by the Si(0Al) signal, the Si/Al ratios for these materials are not very accurate. Therefore, the Si/Al ratios derived from ^{27}Al spectra were used for the calculation of the intrinsic rate constants.[10] The use of the standard ZSM-5 sample without extraframework aluminum makes the analysis of the Al more reliable in this case.

The sodium content (Table 1) for all H forms was less then 0.1 wt % and had a negligible impact on their catalytic properties.[11]

Sorption Equilibria. It was found that the measured isotherms for all materials conform closely to the Langmuir model within an average error of 2% (Figures 1 and 2). The Henry's law constant was derived from the equations

$$N = \frac{N_{max} K_{Lang} p}{1 + K_{Lang} p} \tag{4}$$

and

$$K_{Henry} = K_{Lang} N_{max} \tag{5}$$

Here, K_{Lang} is the Langmuir constant, N_{max} is the saturation limit for *n*-hexane adsorption, N is the measured uptake of *n*-hexane, and p is the partial pressure of *n*-hexane.

The temperature dependence of the Henry constant was assumed to follow the isochoric van't Hoff equation:

$$\left(\frac{\partial \ln K_{Henry}}{\partial \frac{1}{T}}\right)_V = \frac{\Delta U_0}{R} \tag{6}$$

$$K_{Henry} = K_0 \exp\left(-\frac{\Delta U_0}{RT}\right) \tag{7}$$

where ΔU_0 is the adsorption energy and K_0 is the preexponetial factor, which is closely related to the entropy change on adsorption.[12] Since Henry constants represent the initial slope of the adsorption isotherm as coverage tends to 0, the adsorption energy is equal to the limiting isosteric heat of adsorption at zero coverage.

$$\left(\frac{\partial \ln K_{Henry}}{\partial \frac{1}{T}}\right)_V = -\frac{\Delta q_{ist}^0}{R} \tag{8}$$

Henry constants may also be expressed in a volumetric unit, in which the uptake is normalized to the sorption volume of *n*-hexane at 298 K. This volumetric Henry constant indicates the enrichment of the sorbate inside the zeolite pores compared to the sorbate concentration in the gas phase. The volumetric Henry constant, K_{enrich}, will be designated the "enrichment factor" in subsequent discussion.

Na-Zeolites. Adsorption data for the catalytically active, acidic forms of the zeolites are not directly accessible at the reaction temperatures; therefore, the Na forms were chosen to help elucidate the general adsorption properties of *n*-hexane on zeolites at these temperatures. From the van't Hoff plots of the Na forms shown in Figure 3a, the limiting heats of *n*-hexane adsorption in the sodium zeolites were determined in the range 453−623 K, and the results are reported in Table 2. Even though the limiting heat of adsorption for Na−ZSM-5 (the slope of the line in Figure 3a) was larger than that for the H−Y zeolite, the *n*-hexane uptake for the H−Y zeolite exceeded the uptake for the Na−ZSM-5 sample at temperatures above 573 K. The qualitative order for the Henry constants at 623 K is Na−*β* > Na−Y ≥ Na−ZSM-5.

H-Zeolites. From the van't Hoff plots of Figure 3b, it is apparent that the H forms and the Na forms of the zeolites have similar adsorption characteristics with respect to the limiting heats of adsorption and the qualitative order of the enrichment factors. Because of limited catalytic activity, the adsorption equilibrium could be obtained for the H−Y zeolite even at 623 K. Also, subsequent adsorption and desorption cycles did not show any permanent weight gain resulting from possible residual reaction products. For all other zeolites, stable adsorption equilibria could only be obtained below 473 K at all *n*-hexane pressures. At temperatures in the range 473−523 K, *n*-hexane pressures lower than 1 kPa had to be used to avoid reaction. Temperatures higher than 523 K resulted in a permanent weight gain; therefore, these data were not included. For these H-zeolites, the van't Hoff equation was used to extrapolate Henry constants to 623 K. Table 3 summarizes the Henry constants

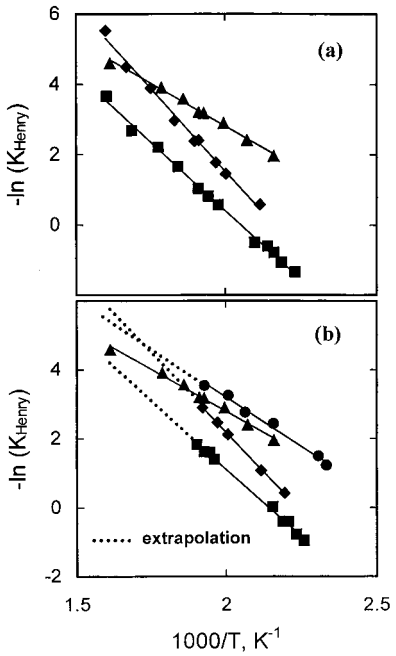

Figure 3. van't Hoff plots showing the temperature dependence of Henry's Law constants for *n*-hexane on (a) Na forms and (b) H forms of (■) β, (◆) ZSM-5, (●) deal. Y, (▲) Y zeolites.

TABLE 2: Heat of Adsorption of *n*-Hexane on the H and the Na Forms of Zeolites ZSM-5, β, Dealuminated Y, and Y

	q_0^{ist} (kJ/mol)	
catalyst	Na form	H form
ZSM-5	78	76
β	65	64
deal. Y		47
Y	43	44

TABLE 3: Henry Constants and Enrichment Factors for n-Hexane in the H and the Na Forms of Zeolites ZSM-5, β, Dealuminated Y, and Y at 623 K

	Na form		H form	
catalyst	K_{Henry} (mmol/g kPa)	K_{enrich}	K_{Henry} (mmol/g kPa)	K_{enrich}
ZSM-5	4.0×10^{-3}	123	3.1×10^{-3}	92
β	2.6×10^{-2}	733	1.6×10^{-2}	430
deal. Y			4.5×10^{-3}	94
Y	1.4×10^{-2}	279	1.0×10^{-2}	198

and enrichment factors for all zeolites at 623 K. Under the same conditions, the H forms adsorbed less *n*-hexane than the Na forms, which suggests that there are specific interactions between the cations and the adsorbate.

The heats of adsorption for the Na form and the H form of the zeolites are reported in Table 2. The value of 76 kJ/mol for ZSM-5 compares favorably with the values of 75−83 kJ/mol reported by Olson et al.[13] The expected difference in the adsorption energy that results from the cation−adsorbate interaction appears to be buried within the experimental error of the technique, which is estimated to be ca. 5%.

Catalytic Results. *High-Pressure Results.* The plots of −ln(1 − conv) versus contact time, shown in Figure 4a for the cracking of *n*-hexane over H−ZSM-5, H−β, and dealuminated H−Y zeolites, are linear over much of the range, which is consistent with first-order kinetics with respect to hydrocarbon concentration. The conversion results also reveal all of the characteristics of a cracking reaction following the bimolecular mechanism.[14,15] From the results obtained over the H−ZSM-5 and deal. H−Y zeolites, it is apparent that the linear behavior

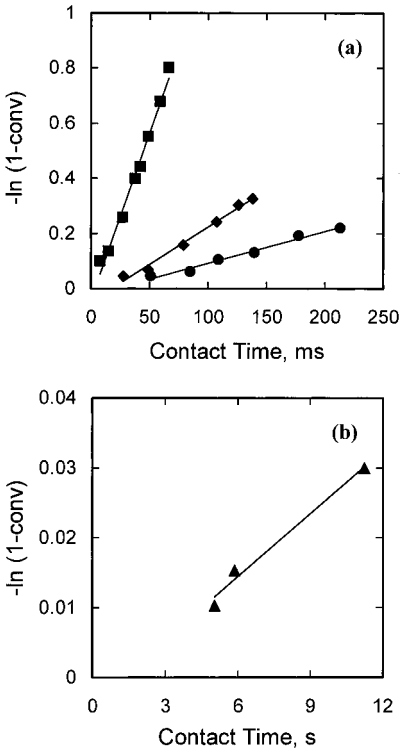

Figure 4. First-order plots for *n*-hexane cracking at $p_{Hex} = 5.3$ kPa and 623 K over (a) (■) H−β, (◆) H−ZSM-5, (●) deal. H−Y, and (b) (▲) H−Y zeolites.

TABLE 4: Paraffin to Olefin Mole Ratios

		p_{Hex} [kPa]	
catalyst	contact time [ms]	0.25	5.7[a]
H−ZSM-5	72	0.81	2.5
H−β	15	0.95	5.6
deal. H−Y	200	0.91	4.9

[a] Paraffin to olefin ratios were determined at 15% for H−ZSM-5, 12% for H−β, and 20% for deal. H−Y.

at longer contact times would not result in a 0 value for ln(1 − conv) at zero contact time; that is, the slopes of the lines describing the data must decrease. At low contact time, the decreasing slopes reflect a smaller bimolecular rate due to a lack of olefins adsorbed on the catalyst surface,[14] which results in negative intercepts for the first-order plots. Others have associated the decreasing slopes with an "induction period" of an autocatalytic reaction in which the olefins required for a bimolecular reaction are produced in a slower monomolecular reaction.[16,17] The high paraffin/olefin ratios (Table 4), the rapid deactivation (Figure 5a) of the catalysts, and the presence of large amounts of isobutane also indicate a bimolecular cracking process. The conversions used to obtain the first-order plots were the extrapolated values at zero time on stream. The experimental data were fit to a third-order polynomial, and the resulting equation was extrapolated to zero time.

In contrast to the dealuminated Y zeolite, which revealed a moderate cracking activity for *n*-hexane cracking, the H−Y zeolite was 2 orders of magnitude less active than all of the other zeolites, as shown in Figure 4b. This relative inactivity of H−Y has been attributed to the presence of Al pairs in next-nearest tetrahedral positions[18,19] and to the absence of extraframework Al.[11,20]

Low-Pressure Results. When the activity tests were carried out at a very low pressure of hexane, the reaction showed a qualitatively different behavior. At sufficiently low conversions

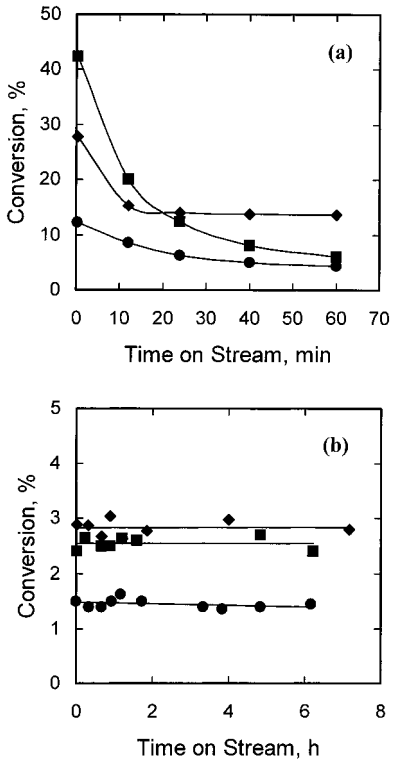

Figure 5. Variation in *n*-hexane cracking with time on stream at (a) $p_{Hex} = 5.3$ kPa, (b) $p_{Hex} \leq 0.5$ kPa at 623 K over (■) H−β, (◆) H−ZSM-5, and (●) deal. H−Y zeolites.

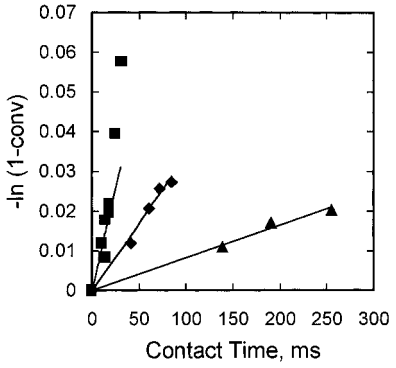

Figure 6. First-order plots for *n*-hexane cracking at $p_{Hex} = 0.25$ kPa at 623 K over (■) H−β, (◆) H−ZSM-5, and (▲) deal. H−Y zeolites.

TABLE 5: First-Order Rate Constants for H−β and H−ZSM-5 Zeolites at 623 K and Low Pressures

	rate, s^{-1}	
p_{Hex} [kPa]	H−β	H−ZSM-5
0.25	1.02	0.34
0.40	0.90	0.36
0.56	0.94	0.29
average	0.95 ± 0.06	0.33 ± 0.04

(<2%), the cracking performance did not change with time on stream for periods longer than 6 h (Figure 5b). Also, no negative intercepts were detectable when −ln(1 − conv) was plotted with respect to contact time (Figure 6), and the calculated rate constants were independent of pressure (Table 5). The paraffin/olefin ratios (Table 4) for all catalysts were less than unity, indicating that hydride transfer was negligible, and the initially formed carbenium ions crack further to smaller olefins via β-scission before the olefin desorbs. In the case of the dealuminated H−Y zeolite, monomolecular conditions could only be obtained at the lowest hexane pressure (0.25 kPa), as indicated by the absence of deactivation of the catalyst. Moreover, the high activity of the H−β zeolite resulted in larger conversions and, thus, more olefins even at relatively short contact times. As a consequence, the bimolecular mechanism became significant at contact times greater than or equal to 25 ms, which is evident by the deviation from a straight line in Figure 6. Table 6 summarizes all measured rate constants under monomolecular and bimolecular conditions.

TABLE 6: Rate Constants Based on Unit Mass or Volume of Catalyst Under Monomolecular ($p_{Hex} = 0.25$ kPa) and Bimolecular ($p_{Hex} = 5.3$ kPa) conditions at 623 K

	k_{mass}[a]		k_{vol}[b]	
catalyst	k^{mono}	k^{bi}	k^{mono}	k^{bi}
H−ZSM-5	0.7	6.1	0.3	2.9
H−β	2.1	28.0	1.0	13.2
deal. H−Y	0.2	1.9	0.1	1.1
H−Y		0.005		0.003

[a] In units of mL g^{-1} s^{-1}. [b] In units of s^{-1}.

TABLE 7: Reaction Pathways and Calculated Rates for H−β, Deal. H−Y, and H−ZSM-5 at $p_{Hex} = 0.25$ kPa and 623 K

		rates (mol/g s × 10^{10}		
	reaction pathways	H−β,[a] 13[b]	H−ZSM-5,[a] 49[b]	H−deal. Y,[a] 129[b]
R1	$C_6H_{14} \rightarrow H_2 + C_6H_{12}$	26	18	9
R2	$C_6H_{14} \rightarrow CH_4 + C_5H_{10}$	0	10	3
R3	$C_6H_{14} \rightarrow C_2H_6 + C_4H_8$	26	47	9
R4	$C_6H_{14} \rightarrow C_3H_8 + C_3H_6$	224	51	23
R5	$C_6H_{14} \rightarrow C_4H_{10} + C_2H_4$	20	10	4
R6	$C_5H_{10} \rightarrow C_3H_6 + C_2H_4$	0	10	0
R7	$C_6H_{12} \rightarrow 2\ C_3H_6$	≥26	≥18	≥9

[a] Catalyst. [b] Contact time (ms).

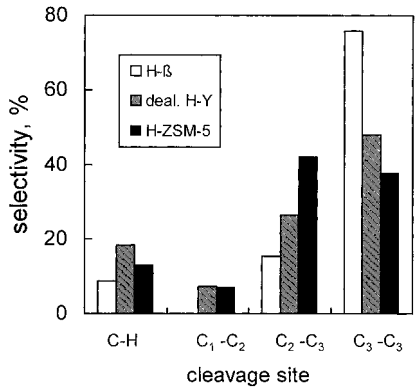

Figure 7. Site selectivity for each cleavage position of the *n*-hexane molecule over H−β, deal. H−Y, and H−ZSM-5 zeolites at $p_{Hex} = 0.25$ kPa and 623 K.

To analyze the mechanism of the low-pressure experiments more thoroughly, the consistency of the product distribution with a simple monomolecular reaction scheme was quantitatively evaluated. The proposed set of reactions that were explicitly used by Narbeshuber et al.[2] for monomolecular *n*-hexane cracking at 773 K are listed in Table 7. In this model, in addition to the possible cracking and dehydrogenation steps, the decomposition of the adsorbed pentene and hexene into ethene and propene is also taken into account. The rates of each reaction, determined from the overall rate of *n*-hexane cracking and the product distribution, are also given in Table 7. The site selectivity, i.e., the fraction of *n*-hexane molecules being cleaved at a particular site, is shown in Figure 7 for the reaction at 623 K. Over the H−β zeolite, *n*-hexane seems to be predominantly cleaved at the central C−C bond, but a more complicated

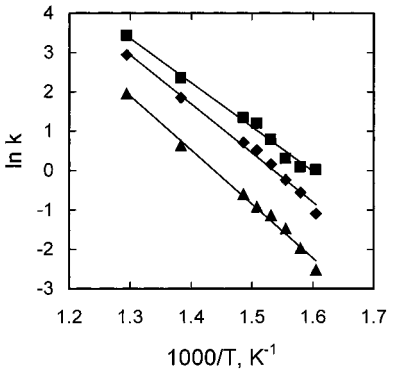

Figure 8. Arrhenius plots for n-hexane cracking at $p_{Hex} = 0.25$ kPa over (■) H−β, (◆) H−ZSM-5, and (▲) deal. H−Y zeolites.

TABLE 8: E_a and E_0 for Monomolecular n-C_6H_{14} Cracking

	kJ/mol	
catalyst	E_a	E_0
H−ZSM-5	108	184
H−β	93	157
deal. H−Y	114	161

cleavage pattern was observed over the H−ZSM-5 zeolite. In this case, the probabilities of cleavage of the *n*-hexane molecule at the C_2-C_3 and C_3-C_3 positions are comparable. There also was significant cleavage at the C_1-C_2 position. The cleavage pattern over dealuminated H−Y was intermediate between those of H−β and H−ZSM-5.

Arrhenius plots shown in Figure 8 are linear for the monomolecular cracking reaction over all three zeolites in the range 623−773 K. This indicates that there is no change in the rate-determining step in this temperature range. The observed activation energies for H−ZSM-5, dealuminated H−Y, and H−β were 108, 114, and 93 kJ/mol, respectively. When the apparent activation energies are corrected for the influence of the heat of *n*-hexane adsorption on these materials (Table 3) and an error of about ±5 kJ/mol is considered, the true activation energies are in the order H−ZSM-5 > dealuminated H−Y ≅ H−β (Table 8). The value of 184 kJ/mol of *n*-hexane cracking over H−ZSM-5 may be compared with values of 197 and 205 kJ/mol reported by Narbeshuber et al.[2] and by Haag,[1] respectively.

No attempt was made to obtain Arrhenius parameters for the bimolecular regime, in part because of the rapid deactivation that occurred with the catalysts. In addition, the bimolecular mechanism involves complex interactions between feed molecules, reaction products (olefins), and catalytically active sites. The apparent activation energies would be of questionable value for interpreting the elementary steps in the catalytic process.

Intrinsic Rate Constants. By combining the adsorption results and the catalytic results, together with the amount of framework aluminum, one can calculate intrinsic rate constants, which reflect the true catalytic performance better than simple conversion data. The apparent rate of n-C_6H_{14} cracking is given by

$$r = k_{app}[n\text{-}C_6H_{14}] \tag{9}$$

If the adsorption of the reactant follows a simple Langmuir isotherm, one can express the rate in terms of the concentration of the reactant within the voids of the zeolite.

$$r = k[n\text{-}C_6H_{14}]_{ads} = k\frac{K_{Lang}[n\text{-}C_6H_{14}]}{1 + K_{Lang}[n\text{-}C_6H_{14}]} \tag{10}$$

TABLE 9: Monomolecular and Bimolecular Intrinsic Rate Constants for H−ZSM-5, H−β, Deal. H−Y, and H−Y Zeolites at 623 K, Based on the Amount of Framework Al

		k_{int}[a]	
catalysts	Si/Al	$k_{int}^{mono} \times 100$	$k_{int}^{bi} \times 100$
H−ZSM-5	35.0	13	111
H−β	16.6	4	51
deal. H−Y	4.7	0.4	6
H−Y	2.5		0.004

[a] In units of s^{-1}.

where K_{Lang} is the Langmuir constant and k is the intrinsic first-order rate constant.

When the *n*-hexane concentration is small enough to be in the linear Henry regime of the isotherm, the above equation can be simplified to

$$r = kK_{enrich}[n\text{-}C_6H_{14}] \tag{11}$$

where K_{enrich} is the enrichment constant and k is the intrinsic first-order rate constant per unit volume of catalyst (in units of s^{-1}), which can be obtained by multiplying the rate constant per unit mass (in units of mL g^{-1} s^{-1}) by the catalyst bed density.

The rate constant, k, depends on the number and strength of the acid sites.[1] To obtain an expression that solely reflects the acid strength of the catalyst (an intrinsic property), one has to correct for the different quantity of active sites, which at first is assumed to be given by the aluminum concentration of the material,[21]

$$r = k_{app}[n\text{-}C_6H_{14}] = k_{int}K_{enrich}\left(\frac{Al}{Al + Si}\right)^{-1}[n\text{-}C_6H_{14}] \tag{12}$$

and therefore

$$k_{int} = \frac{k_{app}}{K_{enrich}}\left(\frac{Al + Si}{Al}\right) \tag{13}$$

where (Al/Al + Si) is the fraction of T-sites occupied by aluminum atoms. The values of K_{enrich} were those reported in Table 2 for the H forms of the zeolite.

The intrinsic rate constants based on the amount of framework Al are summarized in Table 9. The relative order for intrinsic rate constants for both mono- and bimolecular *n*-hexane conversion is H−ZSM-5 > H−β > deal. H−Y ≫ H−Y. For the three active zeolites, the bimolecular rate constant is approximately 1 order of magnitude larger than the monomolecular rate constant. In view of the fact that E_0 is the largest for H−ZSM-5 (Table 8), it is surprising that this catalyst has the largest k_{int}. Perhaps entropy factors associated with the transition state are responsible for the larger rate constant in this zeolite.

The assumption that the number of active (i.e., strongly acidic) sites can be approximated by the framework Al content is probably valid for the H−ZSM-5 and H−β zeolites, but it may not be valid for the dealuminated H−Y material. Infrared spectra in the OH stretching region and catalytic results for partially poisoned zeolites samples, which will be described in a separate publication,[22] show that about 80% of the framework Al content gives rise to active sites for the H−ZSM-5 and H−β zeolites. In the case of the dealuminated H−Y zeolite, only 15% of the framework Al atoms are associated with strongly acidic sites. The result for dealuminated H−Y is consistent with those reported in the literature.[11,23] It is also consistent with the

TABLE 10: Monomolecular and Bimolecular Intrinsic Rate Constants for H−ZSM-5, H−β, Deal. H−Y Zeolites at 623 K, Based on the Fraction of Framework Al That is Associated with Strongly Acidic Sites

		corr. k_{int}[a]	
catalysts	active site/FAL	$k_{int}^{mono} \times 100$	$k_{int}^{bi} \times 100$
H−ZSM-5	0.75	17	148
H−β	0.80	5	64
deal. H−Y	0.15	3	40

[a] In units of s^{-1}.

observation that the protons in a normal H−Y zeolite are largely inactive (Table 9), and a modification of the material is required to generate strong acidity. The requirements for attaining this strong acidity are discussed in detail elsewhere.[19,24−27] Since only 15% of the framework Al atoms are associated with strongly acidic protons, the actual intrinsic rate constant, k_{int}, for dealuminated H−Y is considerably greater than the values listed in Table 9, which implies that the set of most active sites in dealuminated H−Y is almost as active as those in the H−β zeolite. Intrinsic rate constants for H−ZSM-5, H−β, and dealuminated H−Y based on the number of active protons are listed in Table 10. These quantitative values for rate constants are important for studies in which one is attempting to relate cracking activity to acidity as determined by spectroscopic methods, heats of adsorption, etc.

Conclusion

The effect of *n*-hexane adsorption on the rate constants is most clearly evident in a comparison of the values obtained for the H−ZSM-5 and the H−β zeolites. On the basis of gas-phase concentrations and the mass of catalyst, the H−β zeolite appears to be the most active, but if adsorption of *n*-hexane and the framework Al or active site concentration are considered, the intrinsic activity of the H−ZSM-5 zeolite is larger. The true activation energy, however, is the largest for the H−ZSM-5 zeolite. When the number of active protons is considered, based on Na poisoning experiments, the intrinsic activity of the dealuminated H−Y zeolite is about as large as that of the H−β zeolite. These observations will need to be accounted for in theoretical and spectroscopic studies designed to explore the role of acidity in catalytic cracking.

Acknowledgment. This work was sponsored by the National Science Foundation under Grant CHE-9520806.

References and Notes

(1) Haag, W. O. *Stud. Surf. Sci. Catal.* **1994**, *84*, 1375.
(2) Narbeshuber, T. F.; Kinek, H.; Lercher, J. A. *J. Catal.* **1995**, *157*, 388.
(3) Kissin, Y. V. *J. Catal.* **1990**, *126*, 600.
(4) Wang, K. M.; Lunsford, J. H. *J. Catal.* **1972**, *24*, 262.
(5) Sohn, J. R.; DeCanio, S. J.; Lunsford, J. H. *Zeolites* **1986**, *6*, 225.
(6) Lippmaa, E.; Magi, M.; Samoson, A.; Grimmer, A. R.; Engelhard, G. *J. Am. Chem. Soc.* **1980**, *102*, 4889.
(7) Pérez-Pariente, J.; Sanz, J.; Formés, V.; Corma, A. *J. Catal.* **1996**, *124*, 217.
(8) Axon, A.; Klinowski, J. *Stud. Surf. Sci. Catal.* **1989**, *52*, 113.
(9) Man, P. P.; Klinowski, J. *Chem. Phys. Lett.* **1988**, *147*, 581.
(10) Thomas, J. M.; Klinowski, J. *Adv. Catal.* **1985**, *33*, 199.
(11) Fritz, P. O.; Lunsford, J. H. *J. Catal.* **1989**, *118*, 85.
(12) Ruthven, D. M.; Kaul, B. K. *Ind. Eng. Chem. Res.* **1985**, *33*, 199.
(13) Olson, D. H.; Haag, W. O.; Lago, R. M. *J. Phys. Chem.* **1980**, *61*, 390
(14) Haag, W. O.; Dessau, R. M. *Proceedings, 8th International Congress on Catalysis, Berlin 1984*; Dechema: Frankfurt-am-Main, 1984; Vol. 2, p 305.
(15) Riekert, L.; Zhou, J. Q. *J. Catal.* **1992**, *137*, 437.
(16) Santilli, D. S. *Appl. Catal.* **1990**, 60, 137.
(17) Haag, W. O.; Dessau, R. M.; Lago, R. M. *Stud. Surf. Sci. Catal.* **1991**, 60, 255.
(18) Sohn, J. R.; DeCanio, S. J.; Fritz, P. O.; Lunsford, J. H. *J. Phys. Chem.* **1986**, *90*, 4847.
(19) DeCanio, S. J.; Sohn, J. R.; Fritz, P. O.; Lunsford, J. H. *J. Catal.* **1986**, *101*, 132.
(20) Lago, R. M.; Haag, W. O.; Mikovsky, R. J.; Olson, D. H.; Hellring, S. D.; Schmitt, K. D.; Kerr, G. T. *Proceedings of the 7th International Zeolite Conference*; Murakami, Y., Iijima, A., Ward, J. W., Eds.; Kodansha Ltd.: Tokyo, 1986; p 677.
(21) Derouane, E. G.; Andre, J.-M.; Lucas, A. A. *J. Catal.* **1988**, *110*, 58.
(22) Kotrel, S.; Rosynek, M. P.; Lunsford, J. H. To be published.
(23) Lombardo, E. A.; Gustave, A. S.; Hall, W. K. *J. Catal.* **1989**, *119*, 426.
(24) Lunsford, J. H. *ACS Symp. Ser.* **1991**, *452*, 1.
(25) Lónyi, F.; Lunsford, J. H. *J. Catal.* **1992**, *136*, 566.
(26) Beagly, B.; Dwyer, J.; Fitch, F. R.; Mann, R.; Walters, J. *J. Phys. Chem.* **1984**, *88*, 1744.
(27) Barthomeuf, D. *Mater. Chem. Phys.* **1987**, *17*, 49.